Supporting Information

Configurable direction sensitivity of skin-mounted microfluidic strain sensor with auxetic metamaterial

Linna Ma,[a] Taisong Pan,*[ab] Yizhen Ke,[c] Zhuocheng Yan,[a] Sirong Huang,[a] Dengji Guo,[a] Neng Gao,[a] Wen Huang,[c] Guang Yao,[a] Min Gao,[a] Yuan Lin*[abd]

[a] School of Materials and Energy, University of Electronic Science and Technology of China, Chengdu 610054, P.R. China.

[b] State Key Laboratory of Electronic Thin Films and Integrated Devices, University of Electronic Science and Technology of China, Chengdu 610054, P.R. China.

[c] School of Electronic Science and Engineering, University of Electronic Science and Technology of China, Chengdu, 610054, P.R. China

[d] Medico-Engineering Cooperation on Applied Medicine Research Center, University of Electronic Science and Technology of China, Chengdu 610054, P.R. China.

*Corresponding authors.

Email: tspan@uestc.edu.cn (T. P), linyuan@uestc.edu.cn (Y. L)

Note S1: The sensing mechanism of the microfluidic strain sensor

The phenomenological model was based on a previous work of Wood's group.[1] The resistance change of the microfluidic strain sensor with applied strain mainly determines by the change of the length and the cross-sectional area of the microfluidic channel. Two conditions, which are shown in Figure S1, can be considered: 1) axial condition: the tensile strain is applied in the longitudinal direction (ε_x), 2) radial condition: the tensile strain is applied in the transversal direction (ε_y).

In the axial condition, the initial resistance (R_0) of the channel is:

$$R_0 = \rho \frac{l_0}{a_0 b_0} \tag{1}$$

Where ρ is the conductivity of graphene dispersion in the microfluidic channel, l_0 is the length of the channel and $a_0 b_0$ is the cross-sectional area of the channel.

For further derivation, we define the in-plane Poisson's ratio v_{xy}, and the out-of-plane Poisson's ratio v_{yz}. These two Poisson's ratio can be expressed as $\nu_{xy} = -\frac{\varepsilon_y}{\varepsilon_x}$ and $\nu_{yz} = -\frac{\varepsilon_y}{\varepsilon_z}$.

Since the liquid in the channel is incompressible, the volume conservation results in the sum of the strains in the x, y, and z directions leads to zero for small deformation.[2] Consequently, there is an equation:

$$1 - \nu_{xy} - \nu_{yz} = 0 \tag{2}$$

When the device is stretched in the axial condition, the resistance of the device is:

$$R_s = \rho \frac{l_0(1+\varepsilon_x)}{a_0(1-\nu_{xy}\varepsilon_x) b_0(1-\nu_{yz}\varepsilon_x)} \tag{3}$$

Well then, the **Equation S3** is substituted by **Equation S2**, and the new equation is

$$R_s = \rho \frac{l_0(1+\varepsilon_x)^2}{a_0 b_0} = R_0(1+\varepsilon_x)^2 \tag{4}$$

So, the change of device's resistance is:

$$\frac{\Delta R}{R_0} = (1+\varepsilon_x)^2 - 1 \tag{5}$$

Similarly, when the device is stretched in the radial condition, the resistance of the device is:

$$R_s = \rho \frac{l_0(1-\nu_{xy}\varepsilon_y)}{a_0(1+\varepsilon_y)b_0(1-\nu_{yz}\varepsilon_y)} \tag{6}$$

The volume of the channel corresponds with the equation:

$$(1+\varepsilon_y)(1-\nu_{xy}\varepsilon_y)(1-\nu_{yz}\varepsilon_y) = 1 \tag{7}$$

So, the resistance of the device is substituted as:

$$R_s = \rho \frac{l_0(1-\nu_{xy}\varepsilon_y)^2}{a_0 b_0} = R_0(1-\nu_{xy}\varepsilon_y)^2 \tag{8}$$

Therefore, the change of device's resistance in the radial condition is:

$$\frac{\Delta R}{R_0} = (1-\nu_{xy}\varepsilon_y)^2 - 1 \tag{9}$$

Note S2: General model of auxetic metamaterials

Based on the theoretical model proposed by Masters et. al., [3] the in-plane Poisson's ratio of the auxetic metamaterial with the re-entrant cell can be predicted by assuming that deformation of the cellular network occurred by stretching of the atomic bonds and changes in bond angle. The theoretical flexure models of Young's moduli and Poisson's ratio are as below:

$$E_1 = \frac{K_f (h/l + \sin\theta)}{b\cos^3\theta} \tag{10}$$

$$E_2 = \frac{K_f \cos\theta}{b(h/l + \sin\theta)\sin^2\theta} \tag{11}$$

$$\nu_{12} = \frac{\sin\theta(h/l + \sin\theta)}{\cos^2\theta} \tag{12}$$

$$\nu_{21} = \frac{\cos^2\theta}{(h/l + \sin\theta)\sin\theta} \tag{13}$$

$$G_{12} = \frac{K_f (h/l + \sin\theta)}{w(h/l)^2(1 + 2h/l)\cos\theta} \tag{14}$$

Where E_1, E_2, ν_{12}, ν_{21} and G_{12} are the elastic constants for the auxetic frame. E_i being the Young's modulus and G_i being the shear modulus, and v_i being the Poisson's ratio. The force constant K_i is related to the force constants. Among them, the lengths l and h, thickness t, and width w are considered here. This model has been complied with reciprocal relation $E_1\nu_{21} = E_2\nu_{12}$. According to the flexure model, the angle θ between the adjacent bonds determines the value of Poisson's ratio. The frame A1, B1, C1, D1 were designed on the basis of the above theoretical expressions, and calculated based on the Equation S13, therefore the Poisson's ratio decreases as the angle increases in terms of absolute value.

Furthermore, the ν_{21} can be obtained from Gibson's expression and shown in **Equation S15**. The obtained expression about in-plane Poisson's ratio thereby revealing the relationship

with various force constants K_i, which is the thickness and width of the re-entrant cell will affect the stiffness and deformation mechanism, consequently, affect the elastic properties of the entire auxetic metamaterial. When the re-entrant cell is reduced, the Poisson's ratio value under the same angle will be reduced as well. Whereas, the modulation degree of frame A3 obtained by reducing the cell size of frame A1 will be lesser than that of frame A1.

$$\nu_{21} = \frac{-\sin\theta.\cos\theta\left[\frac{1}{K_f}+\frac{1}{K_h}+\frac{1}{K_s}\right]}{(h/l+\sin\theta)\left[\frac{\sin^2\theta}{K_f\cos\theta}+\frac{\sin^2\theta}{K_h\cos\theta}+\frac{\cos\theta}{K_s}\right]} \tag{15}$$

On the basis of Equation S15, the theoretical Poisson's ratio is determined by both the structural (h, l, θ) and material parameters (elastic modulus, stiffness). When the high-modulus auxetic frame (polyimide, thickness: 50 μm, modulus: 2.5 GPa) combined with the low-modulus elastomer (Ecoflex 00-30, modulus: 69 kPa), the modulus ratio and thickness ratio synergistically rearrange the strain distribution of the microchannel, resulting in heterogeneous deformation behaviors. When the device is integrated with the AM and stretched, the strain distribution will be rearranged due to the modulus proportion, as shown in **Figure S11** and **S12**.

Supplementary Figures

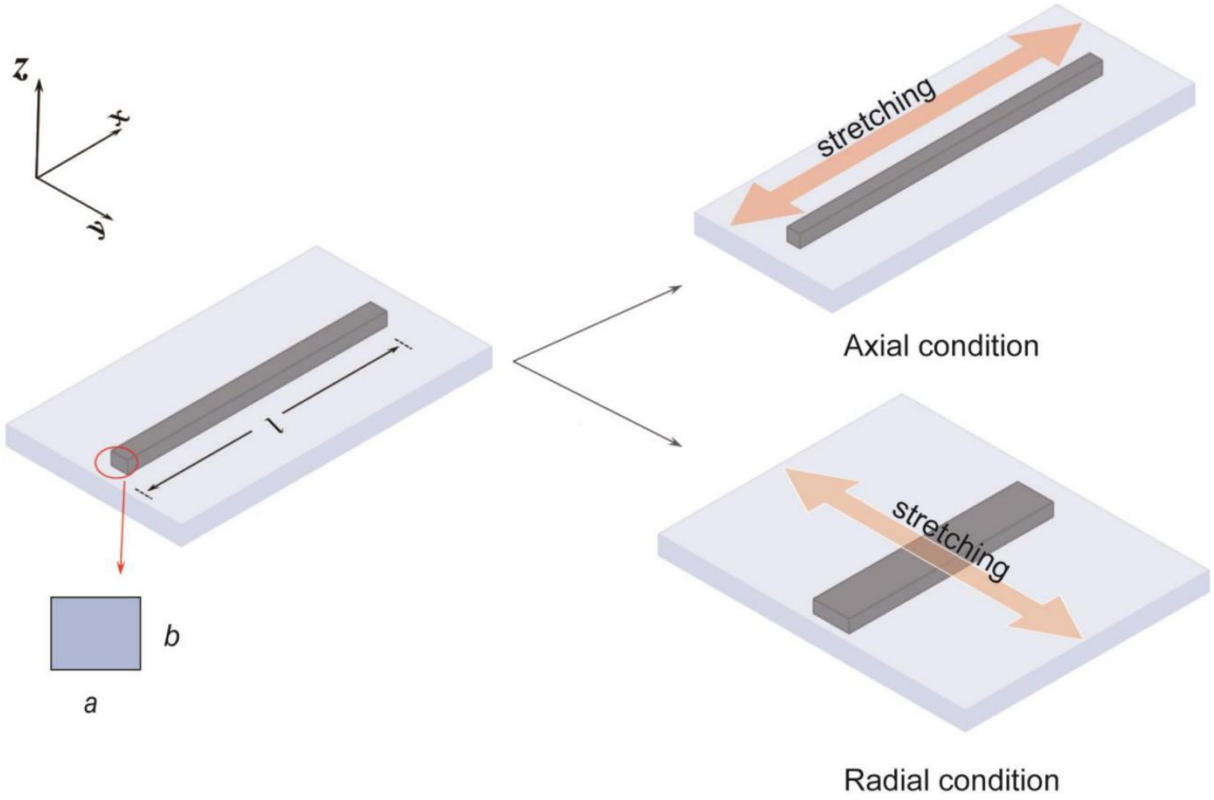

Figure S1. Schematic diagram of the microfluidic strain sensor with two stretching conditions (axial (ε_x) and radial conditions (ε_y)). The applied strains along the length and width of the channel are respectively denoted as ε_x and ε_y.

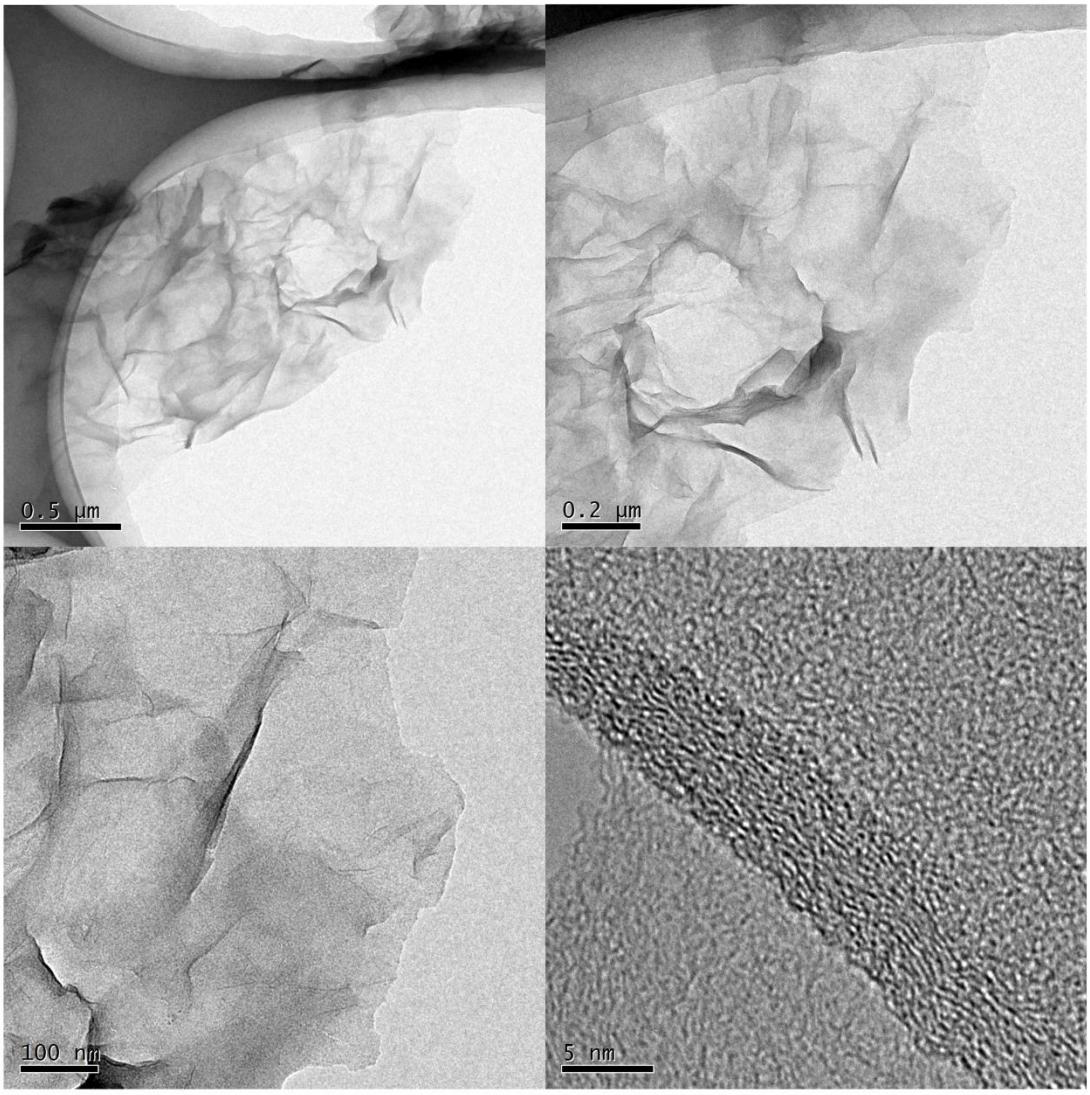

Figure S2. Transmission electron microscopy images of the graphene flakes in the conductive liquid to be filled in the microfluidic channel.

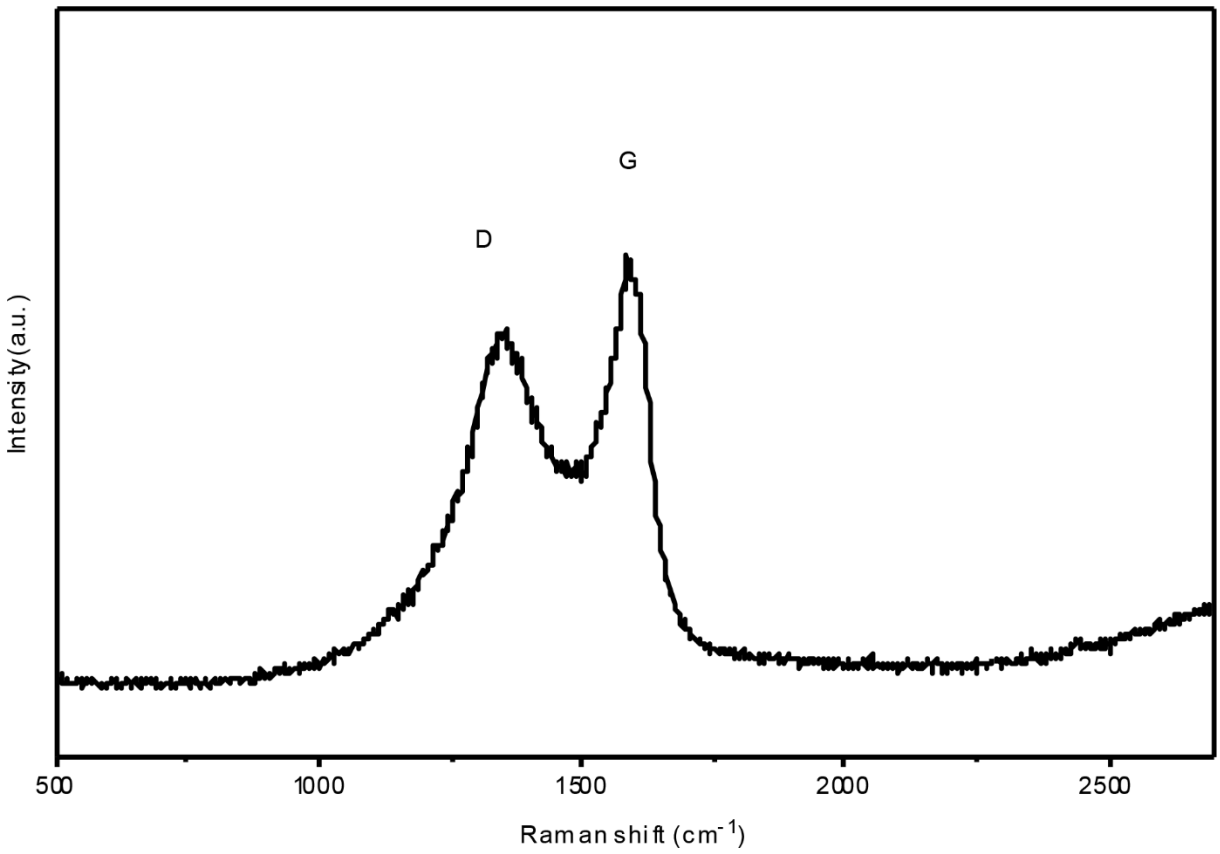

Figure S3. Raman spectrum of the graphene flakes in the conductive liquid to be filled in the microfluidic channel.

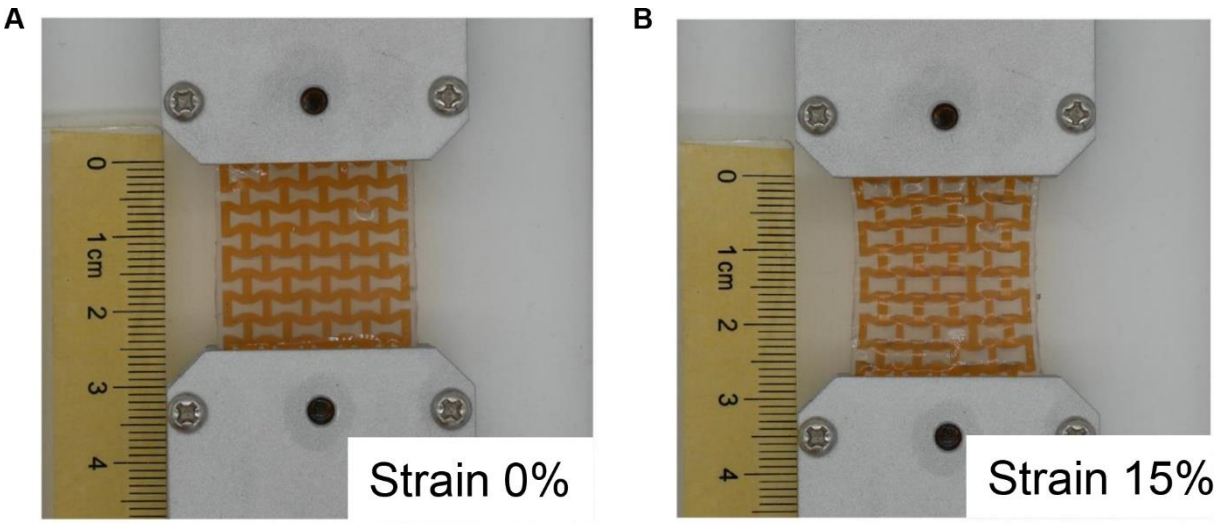

Figure S4. The images of the microfluidic strain sensor with AM frame A1. (a) Initial state; (b) with 15% applied strain in radial condition.

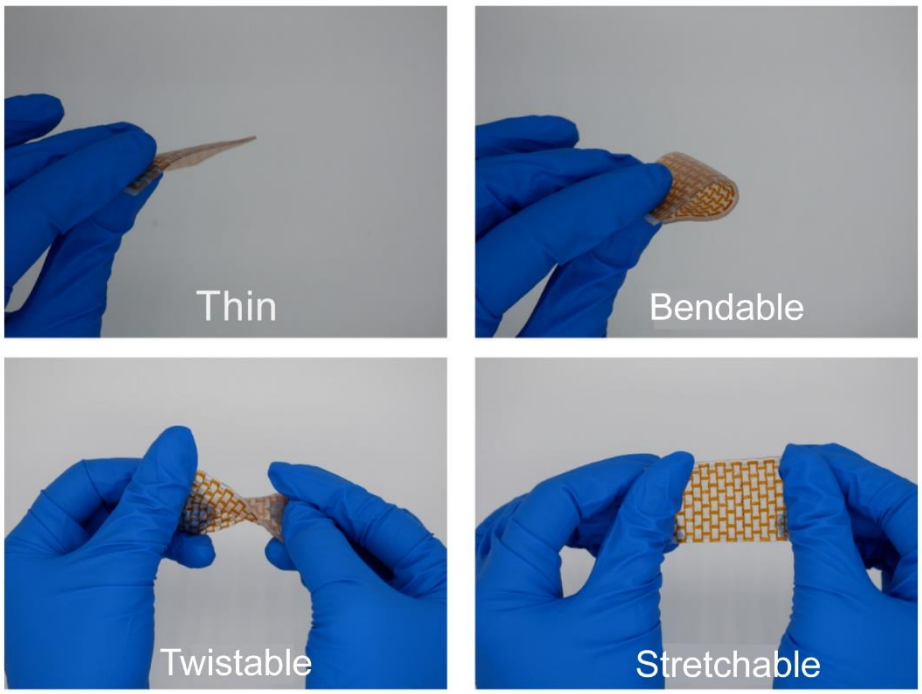

Figure S5. Image of the microfluidic strain sensor with AM.

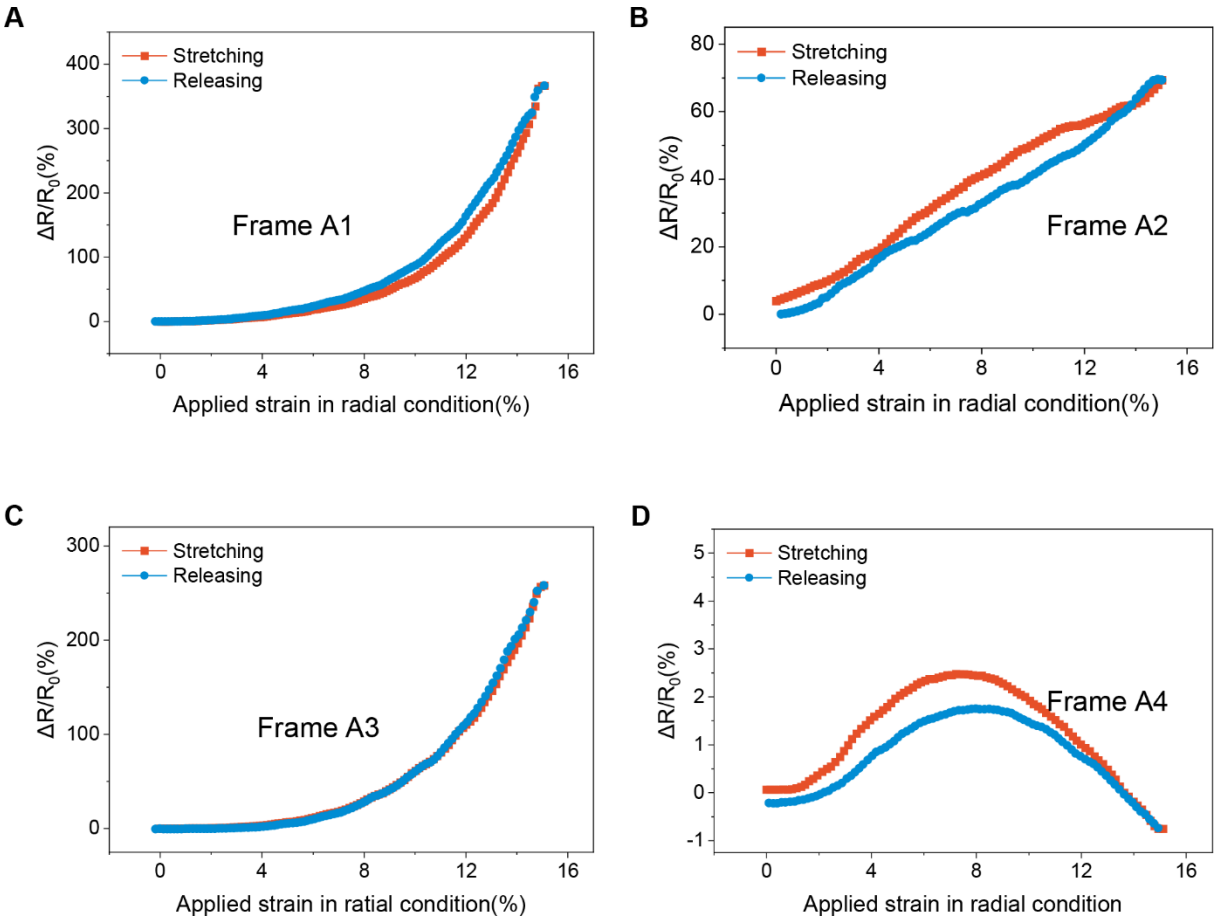

Figure S6. The hysteresis curves of the relative resistive change of microfluidic strain sensors with AM frames A1-A4.

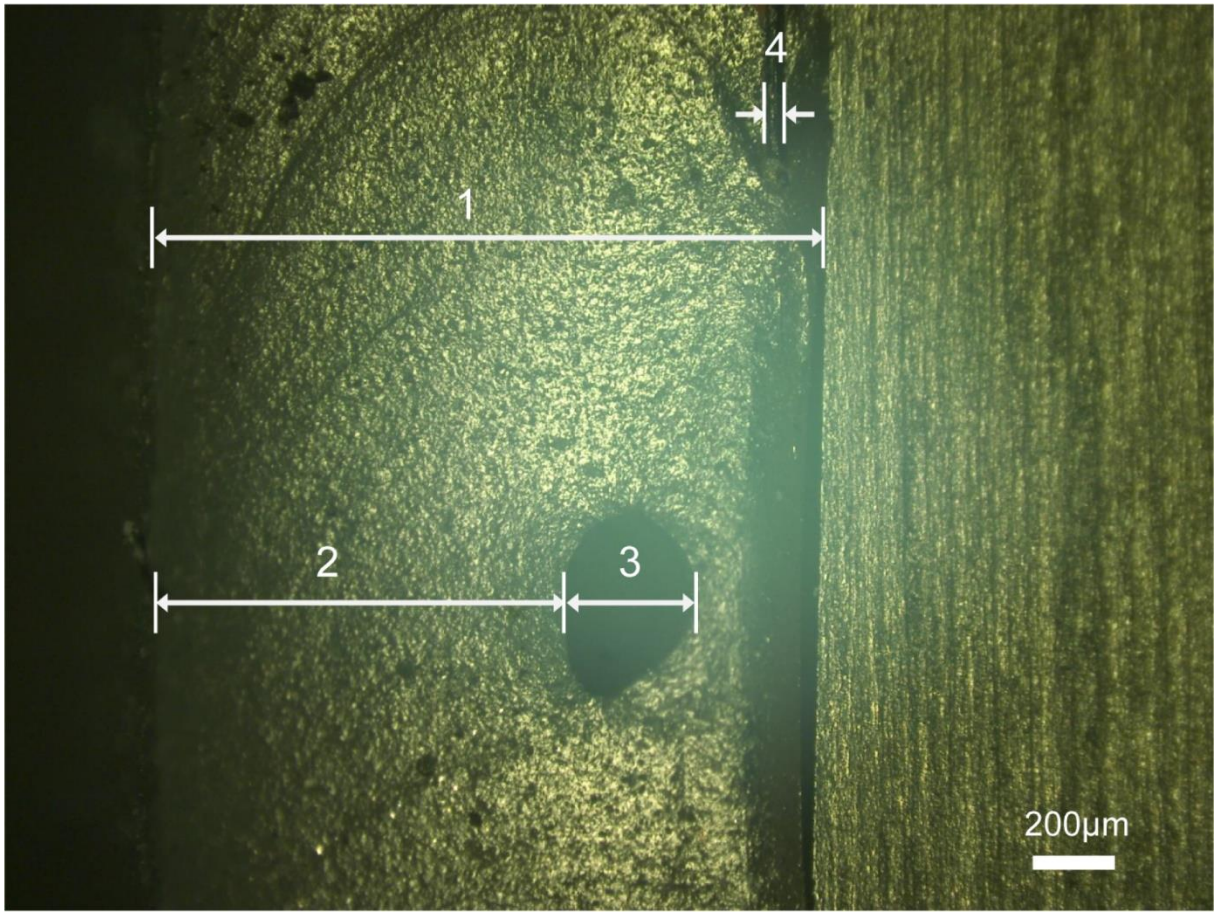

Figure S7. The cross-sectional view of the microfluidic strain sensor with AM, wherein label 1 is the overall thickness, label 2 is the thickness of the upper polymer layer, label 3 is the diameter of the channel, and label 4 is the thickness of the auxetic frame.

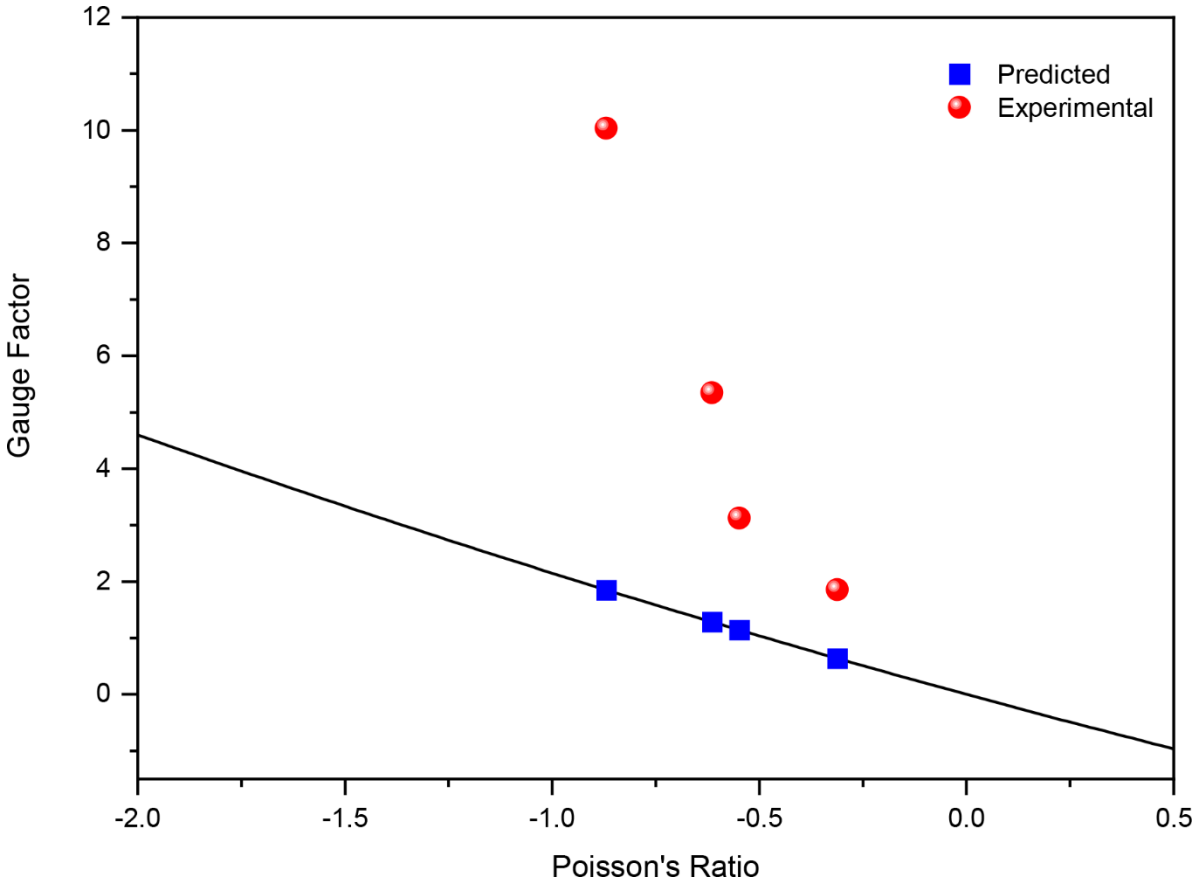

Figure S8. The comparison between the predicted results and experimental results of the dependence of GF on the Poisson's ratio when 15% tensile strain is applied in radial condition. The Poisson's ratio in simulations and experiments is determined by the EPR of the device and Poisson's ratio of AM.

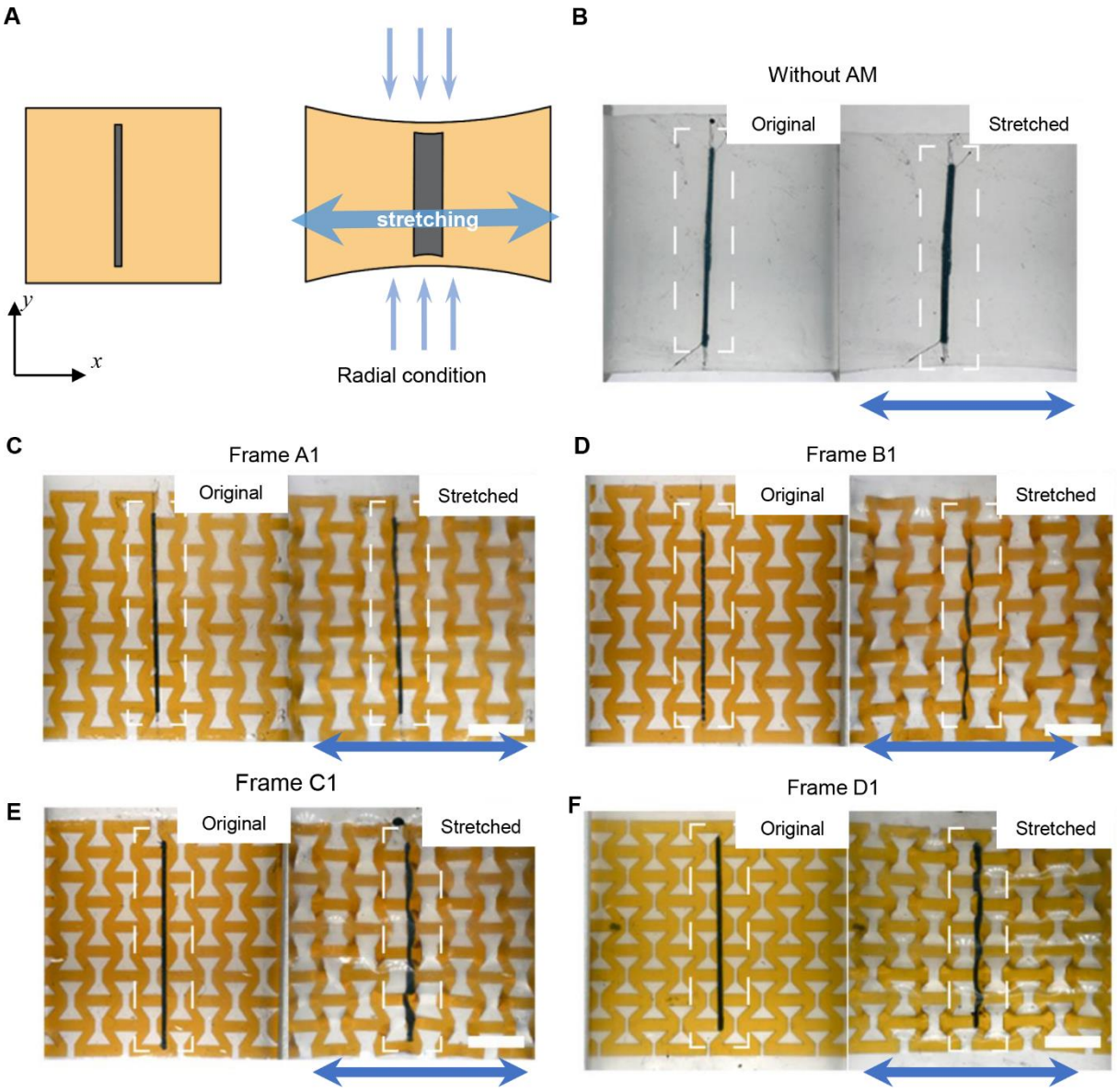

Figure S9. Deformation of the transversal width of the microfluidic channel based on auxetic and conventional structures in radial condition. (a) the directional diagram of the stretched state under conventional structures. (b) Deformation of the transversal width of the microfluidic channel based on conventional structures when applying 15% transversal tensile strain; (c)-(f) Deformation of the transversal width of the microfluidic channel based on different auxetic structures (frame A1, frame B1, frame C1, frame D1) when applying 15% transversal tensile strain.

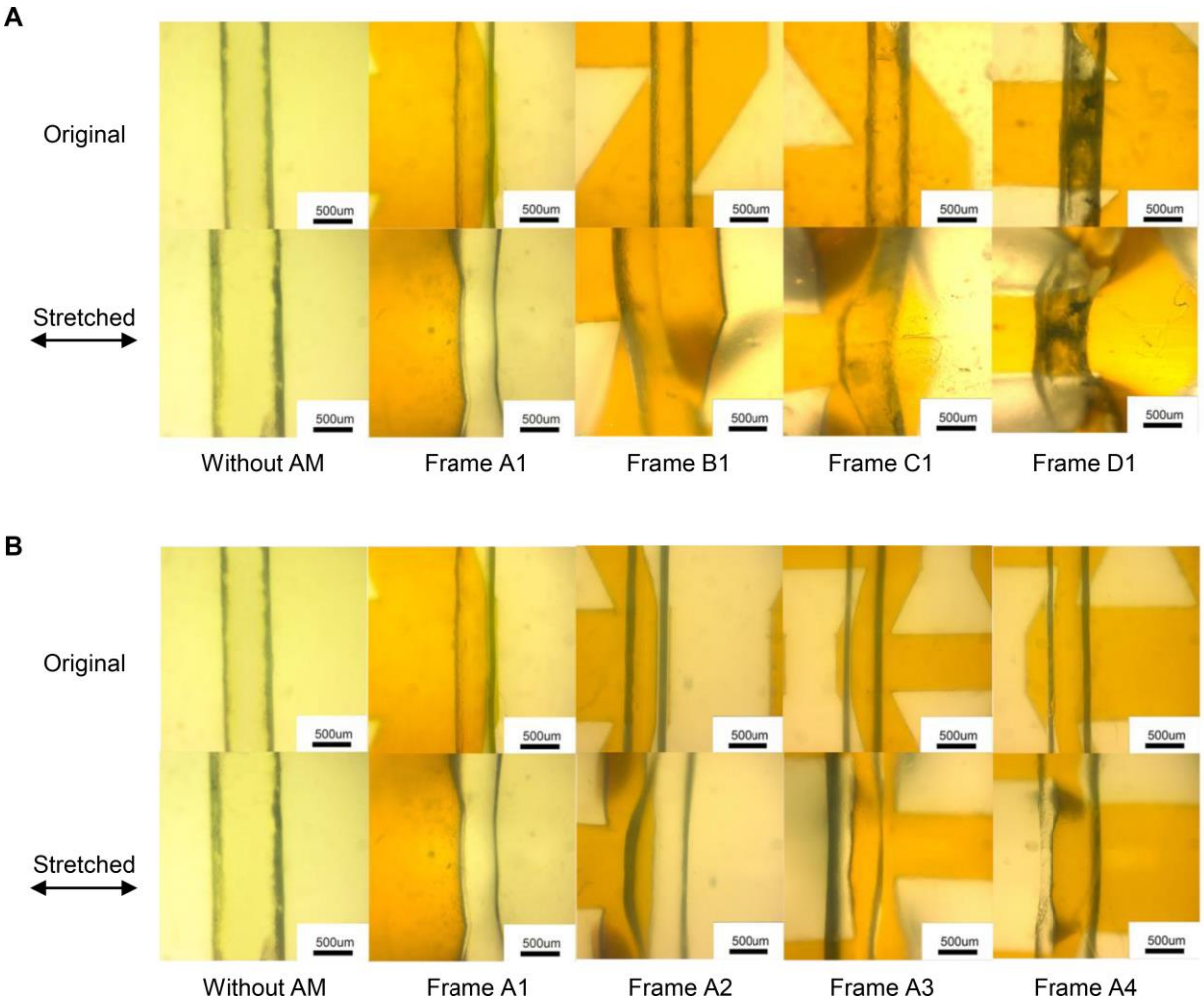

Figure S10. Partial deformation of the transversal width of the microfluidic channel based on auxetic and conventional structures in radial condition (15% tensile strain). (a) Compared with the frame A1-frame D1; (b) Compared with the frame A1-frame A4.

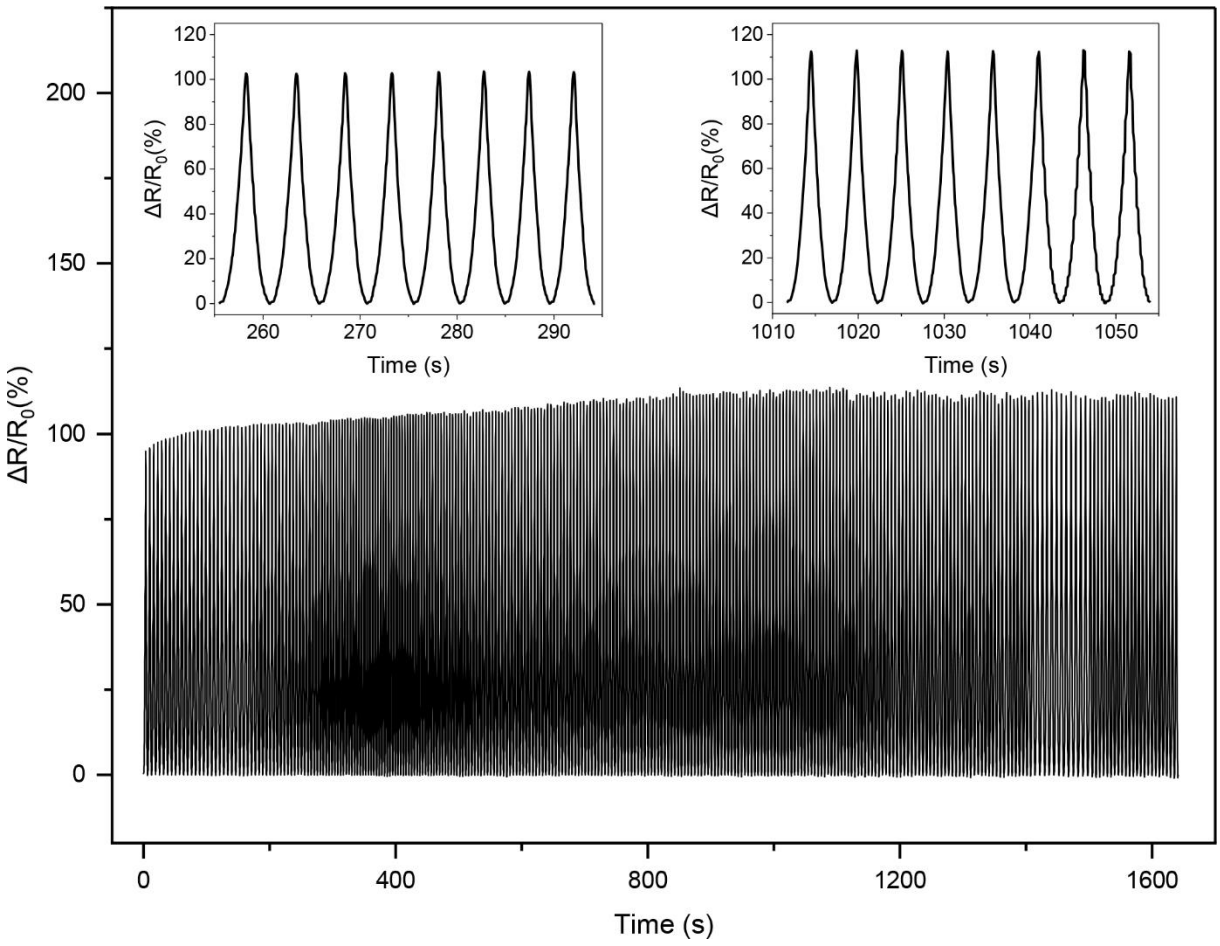

Figure S11. The relative resistance changes of the microfluidic strain sensor with AM (frame A1) under cycle stretching in the radial direction. The applied strain is 10% and the stretching speed is 0.5 cycle/s.

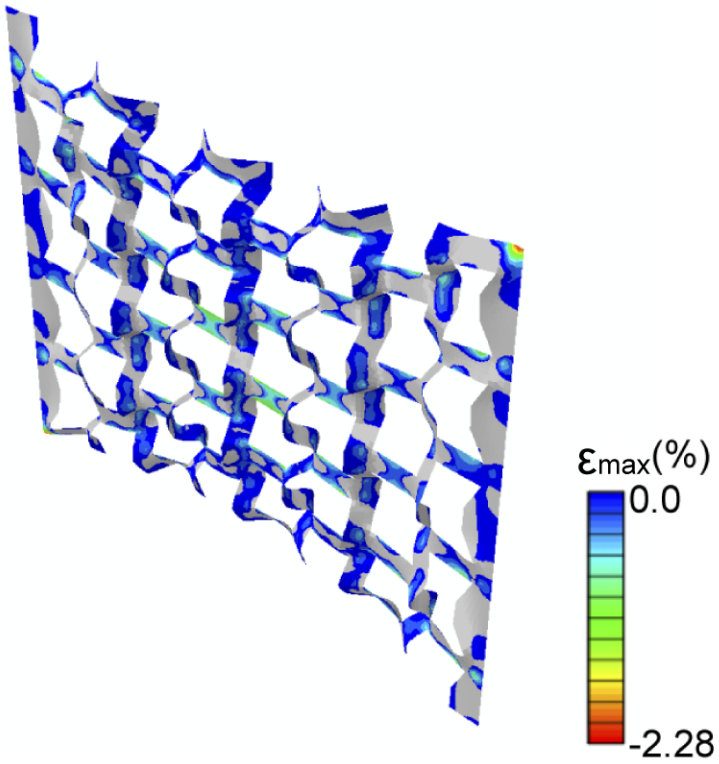

Figure S12. The strain distribution of the auxetic frame (frame A1) is embedded in the bottom layer of the microfluidic strain sensor when applying 15% tensile strain in radial condition. The negative strain value indicates compress strain along the channel and the grey regions indicate the tensile strain along the channel.

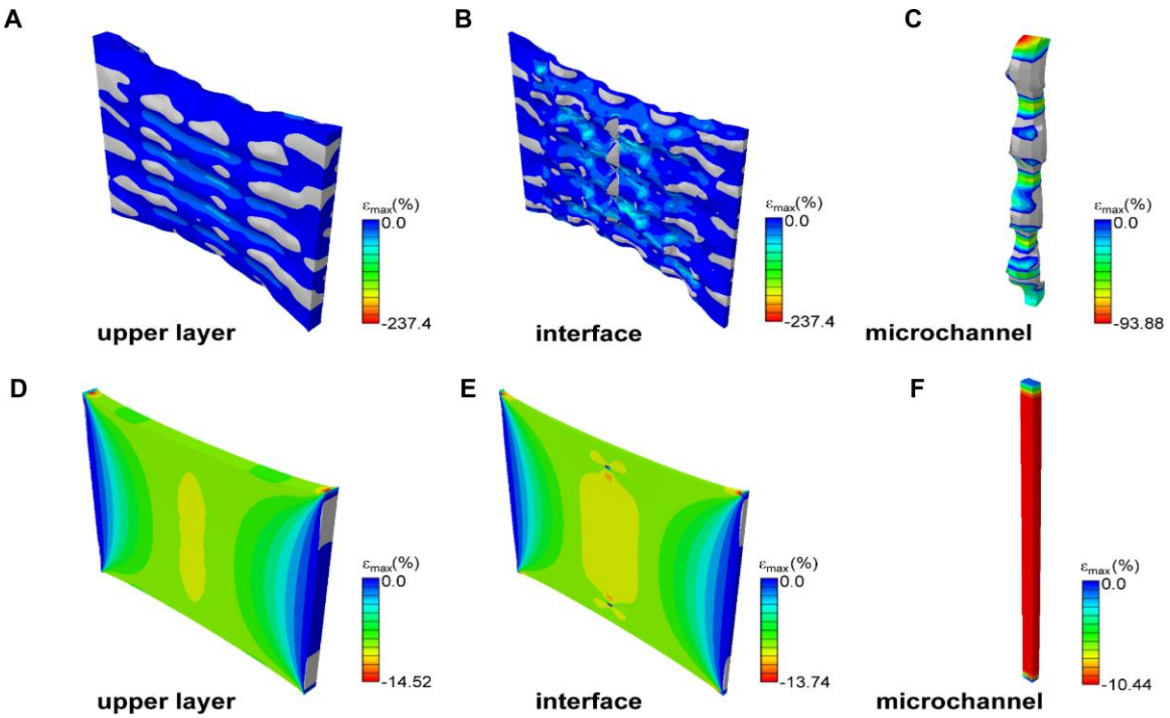

Figure S13. The strain distribution of the microfluidic strain sensor with AM frame A1 in (a) upper layer; (b) interface; (c) channel; The strain distribution of microfluidic strain sensor without AM in (d) upper layer; (e) interface; (f) channel. Two devices are both with 15% tensile strain in radial condition. The negative strain value indicates compress strain along the channel and the grey regions indicate the tensile strain along the channel.

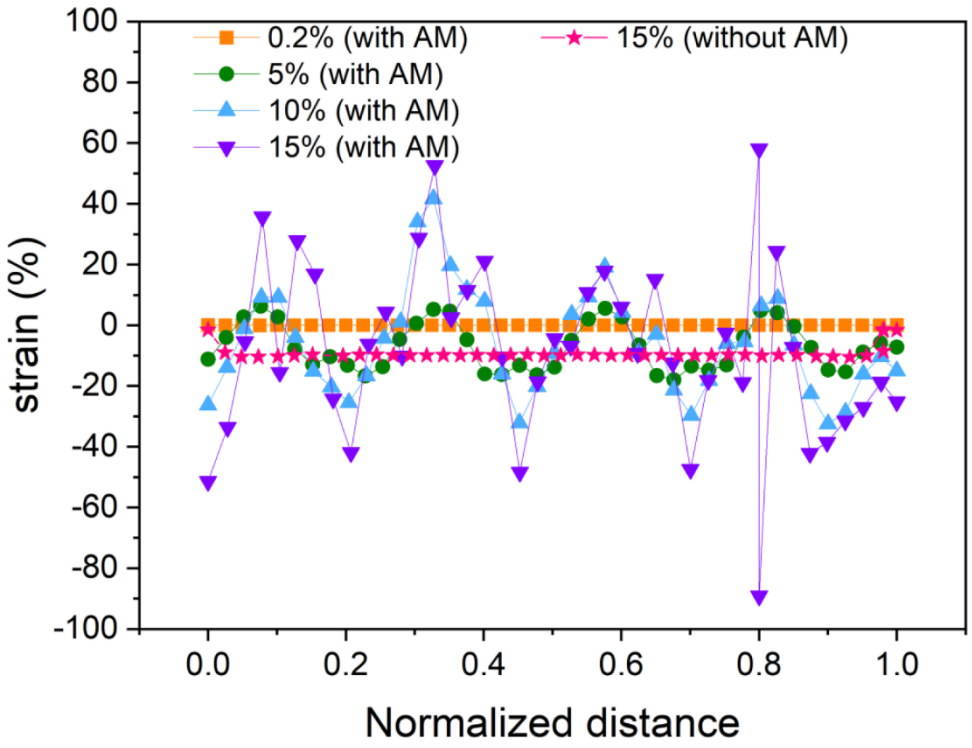

Figure S14. The strain distribution along the channel of the microfluidic strain sensor with AM frame A1) with different applied strains in radial condition.

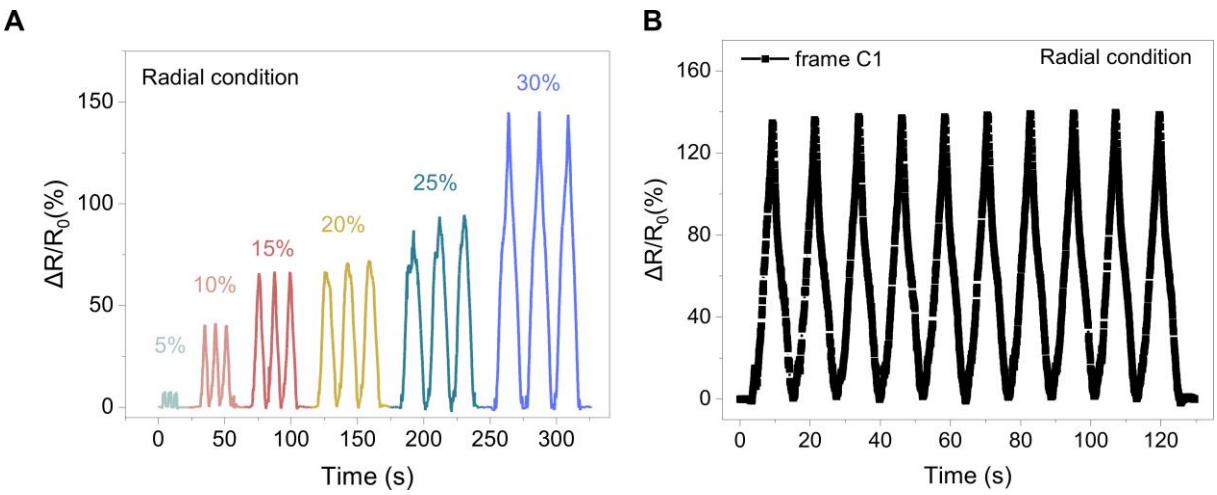

Figure S15. The dynamic response of the microfluidic strain sensor with frame C1 with (a) time-varying strain up to 30% and (b) cyclically applied strain of 30%.

The stretchable range is a microfluidic strain sensor with AM can be expanded to about 30%, which is match the natural range of human skin[4, 5].

Supplementary References

1. S. Xu, D. M. Vogt, W. H. Hsu, J. Osborne, T. Walsh, J. R. Foster, S. K. Sullivan, V. C. Smith, A. Rousing, E. C. Goldfield and R. J. Wood, *Adv. Funct. Mater.*, 2019, **29**, 1807058.
2. Y.-J. Lee, S.-M. Lim, S.-M. Yi, J.-H. Lee, S.-g. Kang, G.-M. Choi, H. N. Han, J.-Y. Sun, I.-S. Choi and Y.-C. Joo, *Extreme Mech. Lett.*, 2019, **31**, 100516.
3. I. G. Masters and K. E. Evans, *Compos. Struct*,. 1996, **35**, 403-422.
4. C. H. Daly and G. F. Odland, *J. Invest. Dermatol.*, 1979, **73**, 84-87.
5. A. P. Gerratt, H. O. Michaud and S. P. Lacour, *Adv. Funct. Mater.*, 2015, **25**, 2287-2295.